

## CORROSION OF IRRADIATED Ni-Mo ALLOYS IN SODIUM FLUORIDE - ZIRCONIUM FLUORIDE MELT

*V.M. Azhazha<sup>1</sup>, A.A. Andriiko<sup>2</sup>, A.S. Bakai<sup>1</sup>, S.V. Volkov<sup>3</sup>, S.V. Devyatkin<sup>3</sup>,  
A.N. Dovbnya<sup>1</sup>, S.D. Lavrinenko<sup>1</sup>, A.A. Omelchuk<sup>3</sup>, B.M. Shirokov<sup>1</sup>, R.S. Shmegeera<sup>3</sup>*  
<sup>1</sup>*National Science Center Kharkov Institute of Physics and Technology, Akademicheskaya str. 1, 61106 Kharkov, Ukraine, e-mail: bakai@kipt.kharkov.ua;*  
<sup>2</sup>*National Technical University "KPI", Department of Chemistry, Pobedy avenue 37, 03056 Kiev-56, Ukraine, e-mail: andriiko@xtf.ntu-kpi.kiev.ua;*  
<sup>3</sup>*Vernadskii Institute of General and Inorganic Chemistry, Ukrainian National Academy of Science, Palladin avenue 32/34, 03680 Kiev 142, Ukraine, e-mail: devyatkin@ionc.kar.net, omelchuk@ionc.kar.net*

The corrosion of nickel-molybdenum alloys and their constituents in a molten eutectic sodium fluoride-zirconium fluoride mixture has been studied by cyclic voltammetry, X-ray analysis, SEM and metallography. The dependence of the corrosion rate of nickel-molybdenum alloys in molten fluorides on the time of soaking in melt and irradiation with an electron beam on an electron accelerator has been investigated. It has been shown that increasing the time of contact of nickel-molybdenum alloys with fluoride melt decreases the corrosion current density, and irradiation increases it in the greater extent the higher the electron beam energy. Intercrystalline corrosion is typical of the alloys of this composition.

### INTRODUCTION

Nickel- and molybdenum- base alloys, which are known as Hastelloy (commercial name), have been widely used in various branches of science and technology, in particular in accelerator-driven nuclear reactors, which operate on molten salt fuel compositions [1]. The development of methods for the control of the corrosion resistance of these alloys to fluoride melts and the elucidation of the effect of different factors (radiation exposure, alloy composition, time of contact with molten salts, etc) on corrosion rate are important not only scientific but also practical tasks since they make it possible to determine the critical service life of structural materials.

This paper presents results of determining the corrosion rate of nickel-molybdenum alloys by cyclic voltammetry in a molten eutectic sodium fluoride-zirconium

fluoride mixture. This mixture is resistant to radioactive irradiation and is recommended as a carrier of isotopes that are to be transmuted in accelerator-driven nuclear reactors. The corrosion resistance of nickel-molybdenum alloys of different composition at different time of contact with fluoride melt under different electron beam irradiation conditions was investigated. The results of estimating the corrosion rate of individual alloy constituents (nickel, molybdenum, iron, niobium, chromium) and the change in the mechanical properties of the alloys under investigation, which has been carried out by nanoindentation analysis, are given [2].

### EXPERIMENTAL

Two alloys of Hastelloy-N type of the following composition (Table 1) were prepared and investigated.

**Table 1**

**Chemical composition of nickel-molybdenum alloys**

Alloy	Chemical composition, wt. %						Other elements
	Ni	Mo	Cr	Fe	Ti	Al	
composition A	base	11...12	6.5...7.5	≤1.5	≤0.5	≤0.8	Mn<0.5; Si<0.15;
composition B	base	11...12	6.2...7.2	≤1.5	≤0.5	≤0.8	Mn<0.5; Si<0.15; Nb-0.5; Y-0.05

The difference in the chemical composition of these alloys was that in the alloys of composition A, 0.3 wt. % chromium was replaced by niobium, and 0.05 wt. % yttrium was added (composition B).

To fabricate the alloys of the chosen composition, the high-purity initial components were used with a low content of interstitial impurities. The basic components of the alloys were nickel, molybdenum chromium, iron,

titanium, niobium, manganese that were refined from undesirable impurities, using the physical techniques.

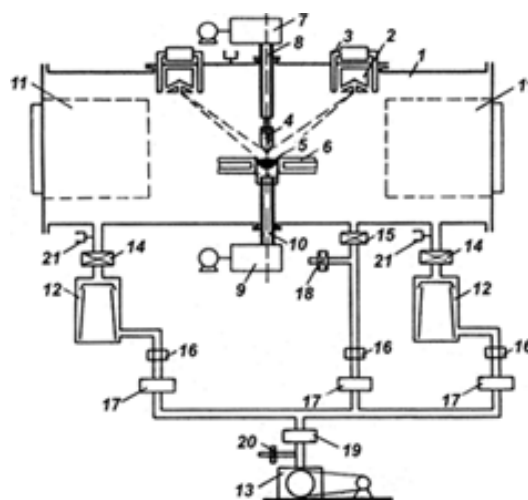
Since those metals have very different properties, it is utterly impossible to remove impurities from them, using only one technique. Refining of nickel, molybdenum, niobium, titanium and iron warranted employment of the electron-beam melting (EBM) technique. Refining of chromium and aluminum made for high-vacuum

annealing. Refining of manganese was made by the vacuum distillation method. The alloy metal component refining resulted in the following information.

**Nickel.** The EBM was made in the ultra-high-vacuum facility “UPM-1” [3,4]. The vacuum system of the facility is composed two diffusion vapor oil pumps with the nitrogen protection and two getter ion pumps “GIN-5”. The boundary vacuum of the facility is  $10^{-6}$  Pa, the vacuum maintained within the limits of  $10^{-2} \dots 10^{-5}$  Pa in the course of the casting. The casting was made via the classic alloy dot-remelting method in the following way: heating>melting>casting> crystallization. Electrolytic nickel was used as initial material that called for double EBM. Schematic of the EBM facility is given in Fig. 1.

In the course of the EBM, the process began of gas release from nickel at different stages of the casting. To monitor the process, the mass-spectrometer “MX-7304A” was used connected to the facility through a device named “Dilutor” [6]. The element composition of the processed nickel and metal upon completion of the EBM was measured, using “EhMAL-2” energy mass-analyzer.

The EBM refinement resulted in production of high-purity nickel samples. The content of the main impurities in nickel samples prior to and after the EBM is given in Table 2.



1. Fig. 1. Schematic of EBM facility, using the oil-free pumping system: 1 – facility frame; 2 – electron beam gun; 3 – bending magnet system; 4 – remeltable electrode; 5 – ingot; 6 – crystallizer; 7, 8 – electrode positioning mechanism; 9, 10 – electrode withdrawal mechanism; 11 – getter ion pump; 12 – diffusion pump; 13 – pre-evacuation pump; 14-20 – vacuum gates; 21 – manometric gauges

Table 2

Content of impurities in initial and post-EBM nickel samples

Impurity, wt. %	Fe	Co	Si	Cu	As	Sb	P	Bi
Initial	0,002	0,0026	0,00003	0,0017	0,00004	0,00003	0,0001	0,00004
Post 2 <sup>nd</sup> EBM	0,0017	0,0009	0,00003	0,0017	0,00001	0,00003	0,00007	0,00004
Impurity, wt. %	Zn	Sn	Al	Pb	Cd	Mg	Se	Cl
Initial	0,0041	0,00005	0,00009	0,00007	0,00005	0,00005	0,0014	0,0005
Post 2 <sup>nd</sup> EBM	0,0008	0,00005	0,00006	0,00007	0,00005	0,00004	0,00027	0,0002

As a result of the refinement, there was a decrease in the content of iron, cobalt, phosphorus, aluminum, magnesium; the content of arsenic, zinc, selenium and chlorine decreased considerably. The double EBM resulted in production of nickel with the purity 99.994 wt. % [4].

The examination of nickel microstructure upon completion of the EBM indicated that it differed substantially from structure of the initial metal. An agglomeration of impurities was observable in nickel after the first remelting on the grain boundaries that was absent after the second EBM re-melting, which bespeaks the effectiveness of nickel refinement, using the EBM.

**Molybdenum.** After the EBM, the content of metal impurities decreased 10-to-30-fold. The removal of silicon was insignificant. Tungsten impurities were not removable. The principal purification was made of the gaseous impurities: oxygen, nitrogen and hydrogen.

**Niobium.** The initial material for the casting was niobium of the brand “NB-1”. The content of metal impurities in niobium after two consecutive EBMs was as follows: Al – 0,004; Fe – 0,0001; Cr < 0,001; Ni < 0,0004; Si – 0,005; Cu – 0,0006; Ca < 0,003 wt. %.

**Titanium.** The initial material for the casting was titanium sponge “TG-90”. A titanium ingot with the purity 99.99 wt.% was produced via the EBM method.

**Iron.** Armco iron rods were used as initial material for the casting. The EBM of iron was carried out via the alloy dot-remelting. The Brinelle hardness of initial Armco iron rods was 830 MPa, decreasing to 624 MPa after the remelting. The iron purity level was determined to a considerable degree by the content of nickel and cobalt.

**Chromium.** The main impurities in chromium were iron, silicon, aluminum, nickel and interstitial impurities

(nitrogen, oxygen and carbon). High-vacuum annealing of chromium samples at the temperature 1200 °C for 5 hours resulted in a decreased content of the interstitial impurities, probably, by 10 times.

In order to introduce the volatile components into the alloy, aluminum and manganese, in a more assured way, the arc casting facility was used priorly to obtain manganese-aluminum alloys.

The voltammetric investigations were carried out in hermetically sealed reactors made of stainless steel under dry argon in a three-electrode electrolytic cell by cyclic voltammetry on a PC controlled potentiostat "Elektroflex" type EF 453. A ZrF<sub>4</sub>(49.5 mol. %)-NaF (50.5 mol. %) melt was used as the electrolyte. The melt was placed in a glassy carbon crucible, which was used as the auxiliary electrode. The working electrodes were samples of Hastelloy (compositions (A and B) heat-treated under different conditions in a molten NaF-ZrF<sub>4</sub> at 650 °C (100...700 hours) and the alloys constituents (Ni, Fe, Mo, Cr, Nb). The potential sweep rate at the working electrode was 10 mV/s. The working electrode potential was recorded with respect to an unpolarized glassy carbon electrode.

Samples of alloys which were subjected in a melt of the above composition to a long (700 hours) irradiation at 650 °C on a LUE-10 (LINAC-10) linear electron accelerator with 10 MeV energy and 5 kW power (current density 0.5 mA/cm<sup>2</sup>) were also investigated.

To assess the effect of electron irradiance on nickel-molybdenum alloys, 6 specimens of alloy of preset composition were put in each ampule made of a carbon-carbon composite filled with a molten eutectic sodium fluoride-zirconium fluoride mixture. The electron beam energy at the entrance to the first sample was estimated to be 5066 eV/atom and at the exit from the last sample 64 eV/atom [5]. Corrosion current at different surfaces of the same sample (electron beam entry-exit) were also estimated. To this end, one of the surfaces of the alloy under investigation was covered with boron nitride paste.

The mechanical investigations were carried out by the nanoindentation method on a Nano Indenter – II device (MTS System) [2].

## RESULTS AND DISCUSSION

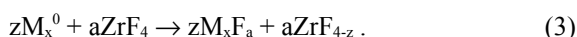
The corrosion rate is determined by metal (Mi) anodic dissolution current:



and can be calculated if the metal (M<sub>y</sub>) ion cathodic reduction current is known:



provided that the total current traversing the cell is zero [6]. Since the experiments were performed in an inert atmosphere, the only cathodic depolarizer (oxidant) in the fluoride melt under investigation can be ions of zirconium or one of the alloy constituents that transferred into the melt by the exchange reaction:



The investigation carried out showed that almost all voltammograms exhibit in the cathodic region a wave which precedes zirconium ion discharge (Fig. 2), therefore the portion of the voltammetric curve (section *ac*) corresponding to the cathodic process at the most positive potential was employed in the calculations of the corrosion rate of the samples under investigation. In the anodic region, all voltammograms exhibited a wave of anodic dissolution of the sample under investigation (section *ab*), which was followed by a current drop (section *bd*, due to a surface passivation) followed by an increase in current (section *df* due to a pit formation). To calculate the corrosion current of the samples under investigation in the anodic region, the initial portion of the voltammetric curve (section *ab*) was used.

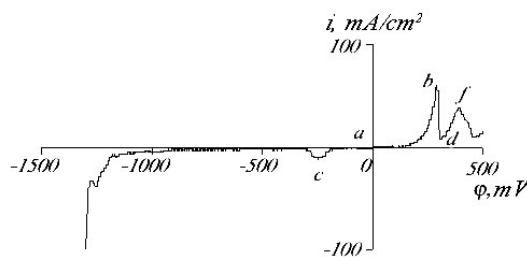


Fig. 2. Voltammogram of a nickel-molybdenum alloy (composition B, sample 120) in a molten eutectic sodium fluoride-zirconium fluoride mixture at 650 °C

Examination of the anodic (section *ab*) and cathodic (section *ac*) branches of voltammograms in semilog coordinates allows one to determine the conditions under which the total current traversing the cell is zero and to calculate the corrosion current density of the sample under investigation (Fig. 3).

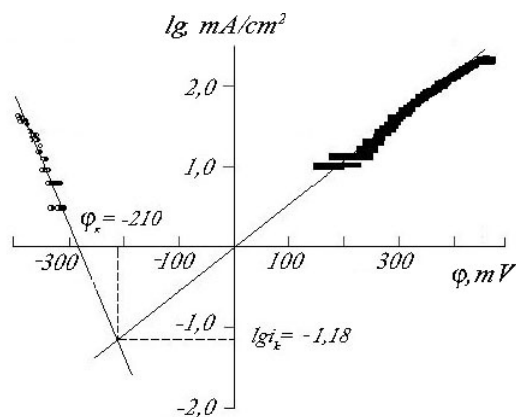


Fig. 3. Calculation of the corrosion current density of a sample of alloy of composition A after 400 hours of isothermal soaking in a sodium fluoride-zirconium fluoride melt at 650 °C

Knowing the corrosion current density, one can calculate the corrosion rate  $K_m = \frac{i_c A_M}{nF}$  (g/m<sup>2</sup>·h) or  $K_k = \frac{K_m}{d_M}$  (mm/yr) [6], where A<sub>M</sub> is the atomic mass of metal, n is the number of electrons involved in the

electrode process,  $F$  is Faraday constant,  $d_M$  is the density of the metal under investigation.

The investigations carried out showed that the current rise on the anodic branch (section *ab*) of voltammograms of nickel-molybdenum alloys is observed in the potential range corresponding to nickel ionization in fluoride melts [7], and that the number of electrons involved in the electrode process is two. Therefore in the calculations of the corrosion rate of these alloys we as-

sumed that  $n=2$ , and that  $A_M$  and  $d_M$  are the atomic mass and density of nickel respectively. An examination of the voltammograms obtained showed that iron ionization is a two-electron process, chromium ionization a three-electron process, niobium ionization a five-electron process, and molybdenum ionization a six-electron process. The results of the calculation of corrosion rates are listed in Table 3.

Table 3

Corrosion rate of nickel-molybdenum alloys and their constituents

Sample	Corrosion current density $i_c, mA/cm^2$	Corrosion rate		Notes
		$K_m, g/m^2 \cdot h$	$K_b, mm/yr$	
Composition A	0.07	0.77	0.76	Without heat treatment
Composition A	0.017	0.19	0.18	After heat treatment
Composition A	0.023	0.25	0.25	100 h of isothermal soaking in a fluoride melt at 650°C without irradiation
—◁—	0.01	0.11	0.11	200 h —◁—
—◁—	0.006	0.066	0.065	500 h —◁—
—◁—	0.00002	0.0002	0.0002	700 h —◁—
Composition B	0.026	0.29	0.28	404 h of isothermal soaking in a fluoride melt at 650°C
Composition A	0.018	0.20	0.19	700 h of isothermal soaking in a fluoride melt at 650°C in the case of irradiation with an electron beam(5066 eV/atom)
Composition A	0.0074	0.081	0.080	—◁— 64 eV/atom
Composition B	0.02	0.22	0.22	—◁— 5066 eV/atom
Composition B	0.0004	0.0044	0.0043	—◁— 64 eV/atom
Mo	0.0016	0.0095	0.008	Without heat treatment
Ni	0.025	0.27	0.27	—◁—
Fe	5.2	54.2	60.37	—◁—
Nb	9.5	107.0	67.47	—◁—
Cr	1000	6466.3	7911.3	—◁—

From the data obtained it follows that the corrosion resistance of the metals investigated decreases in the order: Mo, Hastelloy, Ni, Fe, Nb, Cr. The corrosion rate of Hastelloy (composition A and B) depends on the time of contact with fluoride melt and is the lower the longer the time of isothermal soaking in the melt. This is due to the fact that corrosion products appear at the interface with time, which shift the stationary potential towards more positive values. Besides, the corrosion products formed passivate the surface of the samples under investigation. The surface passivation of Hastelloy is evidenced by the shape of voltammograms in the range of high anodic potential values (Fig. 2). It was noted that the section *df*, which characterizes the presence of pitting corrosion, is found not in all voltammograms. This section is absent on voltammograms of the samples that underwent preliminary heat treatment (Fig. 4, curve 2) and long isothermal soaking in a molten sodium fluoride-zirconium fluoride mixture (Fig. 4, curves 3 and 4).

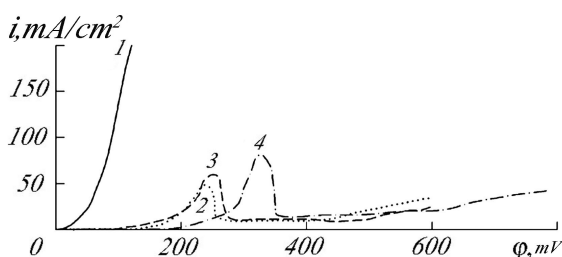


Fig. 4. Voltammograms of Hastelloy (composition A) at different heat treatment conditions: (1) without heat treatment, (2,3,4) after heat treatment: the time of isothermal soaking in a molten eutectic sodium fluoride-zirconium fluoride mixture at 650 °C is 0, 100 and 500 h respectively

The voltammograms of the samples that did not undergo heat treatment exhibit no passivation region (curve 1) even after reaching current densities of over 4 A/cm<sup>2</sup>. The heat treatment sequence and conditions were as follows: heating and soaking for an hour at 1100 °C, water quenching at room temperature, annealing at 675 °C for 50 h under argon. It is non-adherence to the heat treatment conditions that is apparently responsible for the appearance of *df* sections (pitting dissolution), which were found for individual samples of compositions A and B (samples 24, 120, 106).

The samples that were subjected to long electron beam irradiation in a molten eutectic sodium fluoride-zirconium fluoride mixture also retain the passivity region (Fig. 5); it was noted, however, that the potential range with the lowest current density is the narrower the more intense the irradiation to which the samples were subjected.

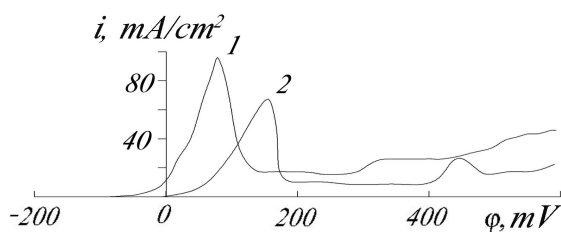


Fig. 5. Voltammograms of Hastelloy (composition A) after irradiation with an electron beam with energy: 1 – 5066 eV/atom; 2 – 64 eV/atom in a molten eutectic sodium fluoride-zirconium fluoride mixture at 650 °C for 700 h

The investigations carried out showed that the voltammetric method enables one to assess the influence of the electron beam irradiance of samples in a fluoride melt. For example, when a sample of composition B is irradiated with an electron beam with an energy of 5066 eV/atom in a fluoride melt at 650 °C for 700h, the corrosion current density is 0.02 mA/cm<sup>2</sup>, and at 64 eV/atom it is 0.0004 mA/cm<sup>2</sup>.

It was noted that the surfaces of the same sample are characterized by different corrosion rates. At the entrance of electron beam to a Hastelloy plate 0,3 mm in thickness, the corrosion current density is on an average an order of magnitude higher than that at the exit. For example, if one of the surfaces of the sample under investigation is coated with boron nitride, and a voltammogram of the uncoated surface is recorded, the corrosion rate at the entrance of electron beam (5066 eV/atom) for the sample of composition B is estimated to be 0,17 mA/cm<sup>2</sup> and at the exit 0,01 mA/cm<sup>2</sup>.

The dependence of the corrosion rate of samples on the heat treatment conditions, the presence of passivation regions in the anodic potential range, and the absence of pronounced pit formation regions allow one to conclude that the corrosion of these alloys is of intercrystalline character. This conclusion agrees with the results of X-ray phase analysis and metallography. According to the results of an X-ray phase analysis, the diffractograms of alloys of compositions A and B, which underwent only the above heat treatment without contact with the molten sodium fluoride-zirconium fluoride mixture, exhibited only the beginning of formation of phases that are high in nickel (low-intensity lines of < 5%) of the intensity of line (111) due to the nickel base with  $d=2.10...2.11$  E ( $Ni_3Mo$  of orthorhombic system) and  $d=1.84...1.88$  E ( $Ni_3(Al,Ti)$  of cubic system). Isothermal soaking in fluoride melts at 650 °C increases the overall annealing (aging) time of the alloy and makes for a change in its structure and appearance of various secondary phases. After isothermal soaking in a fluoride melt for more than 100 h, the secondary phases  $NiAl$ ,  $Ni_2Al_3$ ,  $NiCr$  are identified. The secondary phases manifest themselves most clearly after 500- hour soaking in a fluoride melt. The phase  $Ni_3Mo$  is most discernible in the alloy. In the samples subjected to irradiation in a fluoride melt, only the phase  $Ni_3Mo$  is identified most clearly.

The results of an X-ray phase analysis make it possible in a certain measure to explain the relation between the observed corrosion rates and heat treatment conditions. The alloy sample (Fig. 4, curve 1) not subjected to heat treatment is virtually a homogeneous alloy (solid solution), whose constituents retain individual electrochemical properties, i.e. the alloy constituents with the most negative potential (Al, Ti, Cr, Fe, etc) must dissolve in the first place, and the constituents with more positive electrode potential (Ni, Mo) must accumulate as adatoms on the surface. It was shown above (Figs. 2,3) that the equilibrium potential of the base of the alloy (nickel) is more positive than the alloy corrosion potential (-210 mV). In this case, nickel microcrystals may form on the alloy surface owing to the high mobility of adatoms; these crystals, however, do not create dense homogeneous coating and do not make for its passivation. On the contrary, the alloy corrosion rate must even increase due to the formation of the galvanic couple nickel-metal with a high negative potential (Cr, Fe). The trend of the recorded voltammetric curve (Fig. 4, curve 1) speaks in favor of this corrosion mechanism. Even at high current densities ( $>4$  A/cm<sup>2</sup>), the surface of such a sample does not change to passive state. The results of the X-ray phase analysis showed that the samples of Hastelloy subjected to heat treatment are no longer homogeneous alloys. They are virtually heterophase compositions. The formation of a secondary phase (which is more electronegative relative to the main phase) terminates approximately after 500-hour annealing in a fluoride melt at 650 °C. Since the amount of the secondary phase compounds is small relative to the main phase, and they separate out mainly at the grain boundaries of the main phase, a more stable continuous layer of the base of the alloy remains on the surface after their dissolution. It is this fact that causes the presence of passivation regions in voltammograms, a shift of corrosion potential towards more electropositive values (Fig. 4, curve 4) and hence a decrease in the overall corrosion rate (Table 3). The shift of potential towards more positive values must be the greater the higher the bond energy in the intermetallic compounds formed. According to the results of the X-ray phase analysis, the passivation of the surface is also aided by increase in its adhesion to the sodium fluoride – zirconium fluoride melt. It was noted that after 700-hour contact with the sodium fluoride – zirconium fluoride melt, the phase  $7NaF \cdot 6ZrF_4$  is identified on the surface of all samples. The same effect persists on irradiation with an electron beam.

The results of the voltammetric and X-ray phase investigations agree with the conclusions drawn from metallographic and microscopical analyses (Fig. 6).

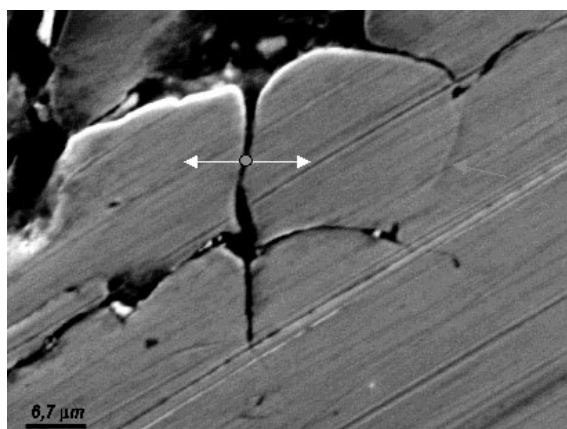


Fig. 6. SEM micrograph: cross-section of a sample of composition A (sample 64) soaked in a NaF-ZrF<sub>4</sub> melt at 650 °C under irradiation with an electron beam of 5066 eV/atom energy for 700 h

Secondary phase compounds are mainly at the grain boundaries of the main phase. On the surface of the samples subjected to electron irradiation there are traces of “etching”. According to the results of SEM, the surface of the sample is destroyed chiefly through the

”etching” of secondary phase compounds at the grain boundaries of the main phase, the etching rate being the higher the higher the electron beam energy. For example, in a sample of composition A (sample 25), the thickness of the damaged layer at the entrance of electron beam (5066 eV/atom) was 60...100 μm and at the exit (opposite side) 40...50 μm. In a sample of composition A (sample 64), the thickness of the damaged layer at the entrance of beam was in the case of irradiation with electron beam with lower energy (64 eV/atom) 15...30 μm and at the exit 10...15 μm. The state of the surface of a sample of composition A (sample 25) at the entrance of electron beam (5066 eV/atom) is shown in Fig. 6. One can clearly see corrosion cracks on the surface of lateral microsection. An X-ray microanalysis has been performed to the right and left of the circle, as shown in the photograph, depthward with a step of 1 μm.

The results are listed in Table 4. The quantitative composition of the sample with coordinate (0 μm) corresponds to the composition on the grain surface but not in the crack. The results obtained allow one to conclude that corrosion damages are mainly of intercrystalline character. The sample is destroyed at grain boundaries, where the melt penetrates. The arrow indicates a future crack.

Table 4

Results of the X-ray microanalysis of the surface of a sample of composition A (sample 24) at the entrance of electron beam (5066 eV/atom) after 700 h at 650 °C in a sodium fluoride-zirconium fluoride melt

Element	Percentage of the alloy constituents (at.%) on the right of crack at a distance of (μm):					
	0	1	2	3	4	6
Ti	0.55	0.44	0.48	0.46	0.62	0.48
Si	0.31	0.25	-	-	0.37	0.36
Cr	7.37	7.62	7.42	7.67	7.95	7.87
Fe	2.35	1.69	1.61	1.74	1.68	1.57
Ni	79.42	78.88	78.26	76.94	77.41	76.87
Mo	4.53	9.11	10.33	11.29	10.66	10.56
Zr	0.58	-	-	0.59	-	-
Percentage of the alloy constituents (at.%) on the left of crack at a distance of (μm):						
Ti	0.45	0.47	0.62	0.60	0.47	0.41
Si	0.41	0.22	0.22	0.34	0.39	0.37
Cr	6.99	7.44	7.86	7.83	7.81	7.70
Fe	1.92	1.66	1.55	1.49	1.68	1.55
Ni	78.89	78.42	77.58	77.33	77.09	77.55
Mo	6.33	9.83	10.40	10.63	10.84	10.74
Zr	0.65	-	-	-	-	-

The nanohardness H and elastic modulus E of the samples under investigation were determined by nanoindentation analysis on a Nano Indenter II device with a Berkovich indenter by the Oliver and Pharr technique [2] from the depth of impression at a maximum load of 10mN (1 gf). The results of the hardness test showed

that either irradiation or salt solutions did not practically affect the mechanical properties of the Hastelloy samples. The results obtained are listed in Table 5. The recommended alloy compositions can be used in the design of molten-salt reactors.

Table 5

Results of the nanoindentation analysis (t=20 °C) of the mechanical properties of Hastelloy

Sample under investigation	Beam energy (eV/atom).	Elastic modulus E, GPa		Nanohardness H, GPa	
		On the surface	In the bulk	On the surface	In the bulk
Sample A after heat treatment	0	266±16	266±16	4.7±0.3	4.7±0.3

Sample A after 700-hour contact with fluoride melt	0	219	219	3.0±2.2	4.9±0.3
	64	242±35	268±8	5.7±0.3	4.8±0.2
	5066	229±35	256±13	5.7±0.5	5.1±0.3
Sample B after heat treatment	0	297±11	297±11	6.9±0.3	6.9±0.3
Sample B after 700-hour contact with fluoride melt	0	251±5	253±6	4.0±0.5	6.9±0.3
	64	240±13	255±7	7.0±0.3	6.9±0.3
	5066	242±17	255±9	6.9±0.2	6.9±0.3

## CONCLUSIONS

The investigations carried out show that intercrystalline corrosion is typical of nickel-molybdenum alloys of the above-mentioned compositions. The corrosion resistance of the investigated samples due to surface passivation is the higher the longer exposure in molten NaF–ZrF<sub>4</sub> mixture. The Hastelloy surface is eroded mainly through the “etching” of the secondary phases at the grain boundaries of the main phase. Surface passivation is not typical of alloys that did not undergo heat treatment.

Irradiation of the alloy surface by 10 MeV an electron beam increases the corrosion rate.

The voltammetric method is useful to control the corrosion resistance of Hastelloy depending on irradiation.

The investigation of the mechanical properties of Hastelloy by nanoindentation analysis show that either irradiation or long contact with fluoride melt did not practically affect their mechanical properties.

Alloys of the proposed compositions can be used in the design of molten-salt nuclear power plants.

## REFERENCES

1.C.D. Bowman. Sustained Nuclear Energy without Weapons or Reprocessing Using Accelerator-Driven System // *Proceedings of the III Intern. Confer. of Accel-*

*erator-Driven Transmutation Technologies*. Praha, June 7–11, 1999.

2.W.C. Oliver and G.M. Pharr, An improved technique for determining hardness and elastic modulus using load and displacement sensing indentation experiments // *J. Mater. Res.* (7). 1992, # 6, p. 1564–1583.

3.G.F. Tikhinsky, G.P. Kovtun, V.M. Azhazha. *Production of ultra high-purity rare metals*. Moscow: “Metallurgy”, 1986, 160 p.

4.V.M. Azhazha, Yu.P. Bobrov, V.D. Vyrych et al. Nickel refinement, using electron beam casting // *Kharkov University bulletin*. Series: “Nuclei, particles, fields”. 2003, # 601, Issue 2(22), p. 118–122.

5.V.M. Azhazha, O.S. Bakai, I.V. Gurin, I.M. Neklyudov, A.O. Omelchuk, V.V. Rozhkov, V.F. Zelenskiy. Study of Corrosion of Construction Materials for Reactors Employing Molten Fluoride Salts or Pb-Bi Coolant Using an Electron Irradiation Test Facility // *Proceedings of the XVI ICPRP, -Alushta, Ukraine, September 6–11, 2004*.

6.L. Kis. *Kinetics of Electrochemical Metal Dissolution*. Budapest: “Akademiai Kiado”, 1988, p. 272.

7.A. Robin and J. de Lepinay. Electrochemical study of the anodic dissolution of Iron and Nickel in molten LiF–NaF–KF eutectic at 600 °C using convolutional voltammetry // *Electrochimica Acta* (37). 1992, #13, p. 2433–2436.

## КОРРОЗИЯ ОБЛУЧЕННЫХ Ni – Mo СПЛАВОВ В РАСПЛАВЕ ФТОРИДОВ НАТРИЯ И ЦИРКОНИЯ

*В.М. Ажажа, А.А. Андрийко, А.С. Бакай, С.В. Волков, С.В. Девяткин, А.Н. Довбня, С.Д. Лавриненко, А.А. Омельчук, Б.М. Широков, Р.С. Шмегера*

Методами циклической вольтамперометрии, рентгенофазового, микроскопического анализов, а также металлографии изучена коррозия никель-молибденовых сплавов и составляющих компонентов в расплавленной эвтектической смеси фторидов натрия и циркония. Исследована зависимость скорости коррозии никель-молибденовых сплавов в расплавленных фторидах от времени выдержки в расплаве и облучения пучком электронов на электронном ускорителе. Показано, что увеличение времени контакта никель-молибденовых сплавов с фторидным расплавом уменьшает плотность тока коррозии, а облучение – увеличивает ее в тем большей мере, чем больше энергия электронного пучка. Для сплавов данного состава характерна межкристаллитная коррозия.

## КОРОЗИЯ ОПРОМІНЕНИХ Ni–Mo СПЛАВІВ В РОЗПЛАВІ ФТОРИДІВ НАТРІЮ ТА ЦИРКОНІЮ

*В.М. Ажажа, О.О. Андрийко, О.С. Бакай, С.В. Волков, С.В. Дев'яткін, О.М. Довбня, С.Д. Лавриненко, А.О. Омельчук, Б.М. Широков, Р.С. Шмегера*

Методами циклічної вольтамперометрії, рентгенофазового, мікроскопічного аналізу, а також металлографії досліджена корозія нікель-молибденових сплавів та компонентів, які входять до їхнього складу, в розплавленій евтектичній суміші фторидів натрію та цирконію. Досліджена залежність швидкості корозії зазначених сплавів від тривалості витри-

мки в розплаві та опромінення пучком електронів на електронному прискорювачі. Показано, що збільшення тривалості контакту нікель-молібденових сплавів з фторидним розплавом зменшує густину струму корозії, а опромінення – збільшує її в тим більшій мірі, чим більша енергія електронного пучка. Для сплавів даного складу характерна міжкристалітна корозія.